

Crystallization of chiral compounds

3.* 3-Phenoxypropane-1,2-diol and 3-(2-halophenoxy)propane-1,2-diols

D. V. Zakharychev, S. N. Lazarev, Z. A. Bredikhina, and A. A. Bredikhin*

A. E. Arbuзов Institute of Organic and Physical Chemistry, Kazan Research Center, Russian Academy of Sciences, 8 ul. Akad. Arbuzova, 420088 Kazan, Russian Federation.

Fax: +7 (843) 273 2253. E-mail: baa@iopc.knc.ru

Specific features of melting of crystalline samples of 3-(2-R-phenoxy)propane-1,2-diols with different enantiomeric compositions were studied by differential scanning calorimetry. The melting points and enthalpies of melting for the racemate and individual stereoisomers were determined. Binary phase diagrams were constructed. The entropy of mixing of individual enantiomers in the liquid phase and the free energy of formation of the racemic compound were calculated. The thermochemical data indicate that the racemates are formed upon the crystallization of phenoxy- and 2-fluorophenoxy-containing compounds, while crystallization of the chloro-, bromo-, and iodo-substituted analogs would form racemic conglomerates.

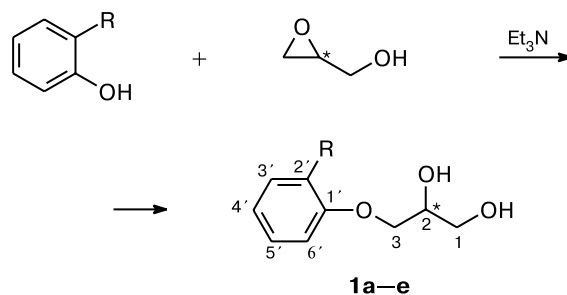
Key words: 3-(2-halophenoxy)propane-1,2-diols, crystallization, racemic conglomerates, thermal analysis, differential scanning calorimetry, phase diagrams, IR spectroscopy.

In the case of chiral compounds, the properties of substances and related materials depend substantially on the enantiomeric composition. Useful properties are usually manifested themselves only when samples with high enantiomeric purity are used. Despite of success achieved in enantioselective synthesis, biotechnology, and preparative chromatography using chiral phases, a considerable (more than 50%) amount of enantiomerically pure substances is produced in industrial scales by the resolution of racemates into individual enantiomers. In this case, methods based on fractional crystallization are prevailing. Among the known methods for racemate resolution, methods based on spontaneous separation during crystallization (spontaneous resolution) play a principal role. This phenomenon² provides racemate separation without auxiliary resolving reagents, chiral phases, *etc.* and/or expensive specialized equipment.^{3,4} A necessary prerequisite for the use of this approach is crystallization of a substance from solution or melt as a racemic conglomerate, *i.e.*, a mechanical mixture of single crystals, each of which is formed by molecules of one configuration only.

The phenomenon of spontaneous resolution has been known for more than 150 years but remains poorly studied, which is caused, first of all, by an insufficient number of the objects investigated. This especially concerns the series of structurally similar molecules in which a small number of variables changes uniformly with substituent replacement. We have recently⁵ found that 3-(2-chlorophenoxy)propane-1,2-diol exhibits a property of sponta-

neous resolution of enantiomers during crystallization. In the structural respect, halogen atoms (including a hydrogen atom) in the role of substituents are similar, being spheres with the successively increasing van der Waals radii (1.2 (H), 1.35 (F), 1.80 (Cl), 1.95 (Br), 2.15 Å (I)). In the present work, we studied specific features of crystallization of of phenyl ethers of glycerol **1a–e** containing the above-listed substituents in the *ortho*-position of the aromatic ring. All substances in the racemic and scalemic forms were synthesized *via* the reaction of the corresponding phenol with racemic or scalemic glycidol (Scheme 1).

Scheme 1



R = H (**a**), F (**b**), Cl (**c**), Br (**d**), I (**e**)

The main method of investigation in this work is differential scanning calorimetry (DSC). The use of this method makes it possible to substantially restrict arbitrariness of measurements of the temperature characteristics of sample melting and to determine quantitatively the

* For Part 2, see Ref. 1.

enthalpies of thermally initiated processes. Based on this quantitative information, one can compare binary phase diagrams of melting constructed experimentally and calculated in different theoretical approximations. Finally, the use of DSC allows one to analyze the thermodynamic characteristics, which are not directly determined in experiments.

Experimental

^1H and ^{13}C NMR spectra were recorded on Bruker MSL-400 spectrometer (^1H , 400 MHz; ^{13}C , 100.6 MHz) using CDCl_3 as solvent, and Me_4Si or signals of the solvent served as the internal standard. Optical rotation was measured on a Perkin-Elmer 341 polarimeter. Specific rotation is given in $\text{deg mL g}^{-1} \text{dm}^{-1}$, and the concentration of solutions appears in g (100 mL)^{-1} .

For usual purposes, melting points were determined on the Boetius heating stage with visual monitoring.

Samples for DSC analysis were prepared by multiple recrystallization and dried in a Fischer apparatus in a vacuum of an oil pump at temperatures by $\sim 5^\circ\text{C}$ lower than the melting point. Chemical purity of samples was monitored by TLC (silica gel, Silufol plates) and GC-MS (Finnigan MAT212 GC-MS spectrometer, column (50 m) with the SE-54 phase, injector temperature 240°C , thermostat temperature $100\text{--}240^\circ\text{C}$, heating rate 6°C min^{-1}). IR spectra of racemic and enantiopure crystalline samples in KBr pellets were recorded on a Bruker Vector 22 spectrophotometer.

Melting curves of samples of 3-(2-*R*-phenoxy)propane-1,2-diols (~ 2 mg) were obtained on a Setaram DSC111 upgraded calorimeter. The calorimeter was equipped with unique systems for controlling a heater and compensating the baseline on the basis of precision analog-to-digital converters,⁶ which increased the effective sensitivity and dynamic range of the instrument. The heating rate was 1°C min^{-1} . Temperature and thermal flux measurements were calibrated by the data for corundum, phenol, and naphthalene. Thermograms were processed by numerical methods using the Mathcad program.* This made it possible to write the processing procedures as standard mathematical formulas, document all procedures with experimental data, and verify and correct experimental data. Discontinuous arrays of experimental data were interpolated by cubic splines and further treated as continuous differentiated and integrated functions, which substantially simplified the procedure of subtraction of the baseline, multiplication by the calibration function, deconvolution, and integration.

(*R*)- and (*S*)-Glycidols (*ee* 91%) were synthesized by the Sharpless enantioselective epoxidation⁷ of allyl alcohol.

Racemic and scalemic diols **1a–e** were synthesized by analogy to a published procedure⁸ from racemic and scalemic glycidols, respectively. (*S*)-Diol was obtained from (*S*)-glycidol, and (*R*)-glycidol gave (*R*)-diol. A mixture of glycidol (0.015 mol, 1.14 g), the corresponding phenol (0.015 mol), triethylamine (0.12 mL, 0.86 mmol), and anhydrous ethanol (3.5 mL) was refluxed for 6 h. After the mixture was cooled down, the solvent was removed, as a rule, under reduced pressure to leave a crys-

talline mixture. A precipitate that formed was filtered off and multiply recrystallized from an appropriate solvent. The physicochemical characteristics of the isolated diols are given below.

rac-3-Phenoxypropane-1,2-diol (1a). The yield was 92%, m.p. $48\text{--}52^\circ\text{C}$ (from ether). A sample of *rac*-**1a** was prepared by the successive recrystallization of the material from ether and CCl_4 followed by the slow evaporation of the solvent from a diol solution in CCl_4 for 1 month, m.p. $56\text{--}60^\circ\text{C}$. A sample with m.p. $60\text{--}74^\circ\text{C}$ was obtained by the further recrystallization of *rac*-**1a** from a hexane–ether (1 : 1) mixture. ^1H NMR, δ : 7.29 (td, 2 H, H(3'), H(5'), $J = 7.4$ Hz, $J = 1.4$ Hz); 6.98 (t, 1 H, H(4'), $J = 7.4$ Hz); 6.91 (dd, 2 H, H(2'), H(6'), $J = 8.4$ Hz, $J = 1.0$ Hz); 4.15–4.08 (m, 1 H, CH_2OH); 4.04 (s, 1 H, CH_2); 4.03 (d, 1 H, CH_2 , $J = 2.1$ Hz); 3.84 (dd, 1 H, CH_2OH , $J = 11.3$ Hz, $J = 3.8$ Hz); 3.75 (dd, 1 H, CH_2OH , $J = 11.7$ Hz, $J = 5.5$ Hz); 2.55 (br.s, 2 H, 2 OH) (see Ref. 9). ^{13}C NMR, δ : 158.55 (s, C(1')); 129.70 (dd, C(2'), C(6'), $^1J_{\text{C,H}} = 158.4$ Hz, $^2J_{\text{C,H}} = 8.7$ Hz); 121.48 (dt, C(4'), $^1J_{\text{C,H}} = 161.3$ Hz, $^2J_{\text{C,H}} = 8.0$ Hz); 114.71 (dm, C(3'), C(5'), $^1J_{\text{C,H}} = 155.5$ Hz); 70.57 (d, C(2), $J = 145.3$ Hz); 69.28 (t, C(3), $^1J_{\text{C,H}} = 144.6$ Hz); 63.83 (t, C(1), $^1J_{\text{C,H}} = 143.9$ Hz).

(*R*)-3-Phenoxypropane-1,2-diol (*R*)-**1a**. The yield was 70%, m.p. $67\text{--}69^\circ\text{C}$ (ether–hexane (1.3 : 1)), $[\alpha]_{\text{D}}^{20} -9.7$ (*c* 1, EtOH), $[\alpha]_{\text{D}}^{20} -8.2$ (*c* 0.5, MeOH) (*cf.* Ref. 10; m.p. $62.5\text{--}64.5^\circ\text{C}$, $[\alpha]_{\text{D}}^{25} -9.5$ (*c* 0.5, MeOH), *ee* 98.9%, Ref. 11; m.p. $56.5\text{--}57^\circ\text{C}$ (EtOH, *ee* 88%), Ref. 12; $[\alpha]_{\text{D}}^{20} -10.8$ (*c* 1, EtOH), *ee* 98%; for (*S*)-**1a** $[\alpha]_{\text{D}}^{20} +10.2$ (*c* 1, EtOH), *ee* 91%). The ^1H and ^{13}C NMR spectra are similar to those published earlier.¹⁰

rac-3-(2-Fluorophenoxy)propane-1,2-diol (rac-1b). The yield was 70%, m.p. $46\text{--}56^\circ\text{C}$ (ether; ether–hexane) (*cf.* Ref. 13; m.p. $56\text{--}57^\circ\text{C}$ (C_6H_6 –petroleum ether)). ^1H NMR, δ : 7.09–6.80 (m, 4 H, Ar); 4.15–4.07 (m, 1 H); 4.04, 4.03–3.95 (s and m, 3 H); 3.81 (dd, 1 H, CH_2OH , $J = 11.5$ Hz, $J = 3.3$ Hz); 3.72 (dd, 1 H, CH_2OH , $J = 11.5$ Hz, $J = 5.7$ Hz); 3.66–3.25 (m, 1 H). ^{13}C NMR, δ : 152.7 (d, C(2'), $^1J_{\text{C,F}} = 245.3$ Hz); 146.6 (d, C(1'), $^1J_{\text{C,F}} = 10.6$ Hz); 124.3 (ddd, C(5'), $^1J_{\text{C,H}} = 162.6$ Hz, $^2J_{\text{C,H}} = 8.8$ Hz, $^4J_{\text{C,F}} = 3.5$ Hz); 121.6 (ddd, C(4'), $^1J_{\text{C,H}} = 164.3$ Hz, $^2J_{\text{C,H}} = 8.2$ Hz, $^3J_{\text{C,F}} = 7.0$ Hz); 116.2 (ddd, C(3'), $^1J_{\text{C,H}} = 162.9$ Hz, $^2J_{\text{C,H}} = 8.2$ Hz, $^2J_{\text{C,F}} = 18.8$ Hz); 115.3 (dd, C(6'), $^1J_{\text{C,H}} = 160.2$ Hz, $^2J_{\text{C,H}} = 8.8$ Hz); 70.6 (t, C(3), $^1J_{\text{C,H}} = 145.0$ Hz); 70.4 (d, C(2), $^1J_{\text{C,H}} = 143.2$ Hz); 63.46 (t, C(1), $^1J_{\text{C,H}} = 142.6$ Hz).

(*S*)-3-(2-Fluorophenoxy)propane-1,2-diol ((*S*)-**1b**). The yield was 72%, m.p. $45\text{--}57^\circ\text{C}$ (CHCl_3). After several successive recrystallizations from CCl_4 and C_6H_6 and double recrystallization from a C_6H_6 –hexane (1 : 1) mixture, a sample of diol (*S*)-**1b** with m.p. $54\text{--}60^\circ\text{C}$ was obtained, $[\alpha]_{\text{D}}^{20} +6.4$ (*c* 1, EtOH).

rac-3-(2-Chlorophenoxy)propane-1,2-diol (rac-1c). The yield was 65%, m.p. $70\text{--}80^\circ\text{C}$ (CCl_4 ; CH_2Cl_2 –hexane (1 : 1)) (*cf.* Ref. 14; m.p. $71\text{--}72^\circ\text{C}$ (petroleum ether– C_6H_6)). ^1H NMR, δ : 7.35 (dd, 1 H, H(6), $J = 7.2$ Hz, $J = 1.4$ Hz); 7.20 (td, 1 H, H(8), $J = 7.8$ Hz, $J = 1.2$ Hz); 6.92 (d, 1 H, H(9), $J = 7.9$ Hz); 6.92 (t, 1 H, H(7), $J = 7.2$ Hz); 4.17–4.05 (m, 3 H, CH_2 , CH); 3.90–3.77 (m, 2 H, CH_2OH); 3.20 (d, 1 H, CHOH , $J = 4.3$ Hz); 2.66 (t, 1 H, CH_2OH , $J = 5.7$ Hz) (*cf.* Ref. 9). ^{13}C NMR, δ : 153.90 (m, C(1')); 130.23 (dd, C(3'), $^1J_{\text{C,H}} = 164.3$ Hz, $^2J_{\text{C,H}} = 8.7$ Hz); 127.82 (dd, C(5'), $^1J_{\text{C,H}} = 161.2$ Hz, $^2J_{\text{C,H}} = 9.7$ Hz); 122.95 (m, C(2')); 122.04 (dd, C(4'), $^1J_{\text{C,H}} = 163.3$ Hz, $^2J_{\text{C,H}} = 7.6$ Hz); 113.76 (dd, C(6'), $^1J_{\text{C,H}} = 159.7$ Hz,

* ©Mathsoft Engineering and Education Inc., <http://www.mathsoft.com>.

$^2J_{C,H} = 8.7$ Hz); 70.71 (t, C(3), $^1J_{C,H} = 145.2$ Hz); 70.10 (d, C(2), $^1J_{C,H} = 145.5$ Hz); 63.62 (t, C(1), $^1J_{C,H} = 142.9$ Hz).

(R)-3-(2-Chlorophenoxy)propane-1,2-diol ((R)-1c). The yield was 60%, m.p. 90–92 °C (CCl₄; twice from CH₂Cl₂), $[\alpha]_D^{20} +13.3$ (c 1, hexane–EtOH (4 : 1)) (cf. Ref. 8: m.p. 91.8 °C (EtOH, determined by DSC), Ref. 15 for (S)-1c: m.p. 87–89 °C, Ref. 12: $[\alpha]_D^{20} +14.0$ (c 1, hexane–EtOH (4 : 1)), ee 99%; for (S)-1c $[\alpha]_D^{20} -13.4$ (c 1, hexane–EtOH (4 : 1)), ee 99%). The ¹H NMR spectrum is similar to that presented in the earlier published work.¹⁵

rac-3-(2-Bromophenoxy)propane-1,2-diol (rac-1d). The yield was 70%, m.p. 84–101 °C (CH₂Cl₂) (cf. Ref. 16: m.p. 82–83 °C (C₆H₆–petroleum ether)). ¹H NMR, δ: 7.53 (dd, 1 H, H(3'), $J = 7.9$ Hz, $J = 1.7$ Hz); 7.26 (td, 1 H, H(5'), $J = 7.8$ Hz, $J = 1.1$ Hz); 6.91 (dd, 1 H, H(6'), $J = 8.2$ Hz, $J = 1.4$ Hz); 6.87 (td, 1 H, H(4'), $J = 7.5$ Hz, $J = 1.2$ Hz); 4.18–4.07 (m, 3 H, CH₂, CH); 3.91–3.80 (m, 2 H, CH₂OH); 3.05 (d, 1 H, CHOH, $J = 4.8$ Hz); 2.48 (t, 1 H, CH₂OH, $J = 6.2$ Hz). ¹³C NMR, δ: 154.70 (m, C(1')); 133.28 (dd, C(3')), $^1J_{C,H} = 164.5$ Hz, $^2J_{C,H} = 8.4$ Hz); 128.60 (dd, C(5')), $^1J_{C,H} = 161.2$ Hz, $^2J_{C,H} = 8.7$ Hz); 122.56 (dd, C(4')), $^1J_{C,H} = 163.5$ Hz, $^2J_{C,H} = 7.9$ Hz); 113.58 (dd, C(6')), $^1J_{C,H} = 159.7$ Hz, $^2J_{C,H} = 8.7$ Hz); 112.28 (m, C(2')); 70.82 (t, C(3), $^1J_{C,H} = 145.2$ Hz); 70.03 (d, C(2), $^1J_{C,H} = 145.0$ Hz); 63.62 (t, C(1), $^1J_{C,H} = 142.7$ Hz).

(R)-3-(2-Bromophenoxy)propane-1,2-diol ((R)-1d). The yield was 56%, m.p. 101–102 °C (CH₂Cl₂), $[\alpha]_D^{20} +13.8$ (c 1, hexane–EtOH (4 : 1)), $[\alpha]_D^{20} -9.0$ (c 1, CHCl₃) (cf. Ref. 17: m.p. 98 °C (PrⁱOH), $[\alpha]_D^{22} -9.7$ (c 1.08, CHCl₃), ee 100%). The ¹H and ¹³C NMR spectra are similar to those presented in Ref. 17.

rac-3-(2-Iodophenoxy)propane-1,2-diol (rac-1e). The yield was 80%, m.p. 90–92 °C (CH₂Cl₂). After repeated recrystallization from the same solvent, the product with m.p. 90–106 °C was obtained (cf. Ref. 18: m.p. 95 °C (CHCl₃)). ¹H NMR, δ: 7.77 (dd, 1 H, H(3'), $J = 7.9$ Hz, $J = 1.4$ Hz); 7.31 (td, 1 H, H(5'), $J = 7.8$ Hz, $J = 1.1$ Hz); 6.84 (dd, 1 H, H(6'), $J = 8.1$ Hz, $J = 1.3$ Hz); 6.75 (td, 1 H, H(4'), $J = 7.6$ Hz, $J = 1.0$ Hz); 4.17–4.07 (m, 3 H, CH₂); 3.90, (dd, 1 H, CH₂OH, $J = 11.7$ Hz, $J = 3.8$ Hz); 3.85 (dd, 1 H, CH₂OH, $J = 11.7$ Hz, $J = 4.5$ Hz); 2.26 (br.s. 2 H, 2 OH). ¹³C NMR, δ: 156.94 (m, C(1')); 139.43 (dd, C(3')), $^1J_{C,H} = 165.2$ Hz, $^2J_{C,H} = 10.0$ Hz); 129.66 (dd, C(5')), $^1J_{C,H} = 161.2$ Hz, $^2J_{C,H} = 8.6$ Hz); 123.33 (dd, C(4')), $^1J_{C,H} = 163.2$ Hz, $^2J_{C,H} = 8.0$ Hz); 112.65 (dd, C(6')), $^1J_{C,H} = 159.9$ Hz, $^2J_{C,H} = 8.6$ Hz); 86.80 (m, C(2')); 70.95 (t, C(3), $^1J_{C,H} = 145.3$ Hz); 70.10 (d, C(2), $^1J_{C,H} = 143.3$ Hz); 63.68 (t, C(1), $^1J_{C,H} = 143.3$ Hz).

(S)-3-(2-Iodophenoxy)propane-1,2-diol ((S)-1e). The yield was 72%, m.p. 111–113 °C (CH₂Cl₂), $[\alpha]_D^{20} -15.9$ (c 1, hexane–EtOH (4 : 1)).

Results and Discussion

A known indication for formation of a racemic substance by a chiral compound in the solid phase is discrepancy of vibrational spectra of solid enantiomerically pure and racemic samples.^{19,20} We compared the IR spectra of

similar pairs of aromatic glycerol ethers **1a–e**. To substantiate the comparison, the spectra were subjected to a procedure of normalization and baseline correction. For this purpose, coefficients that minimize the difference $A_s - [a_0 + a_1\nu + A_r(a_2 + a_3\nu)]$, where A_s and A_r are the molar absorption coefficients of the scalemic and racemic samples, respectively; ν is the IR radiation frequency corresponding to A , and a_n are the desired regression coefficients, were selected by the least-squares method. It is reasonable to introduce the regression terms $a_1\nu$ and $a_3A_r\nu$ to correct spectral differences caused by the nonspecific (not related to particular absorption bands) interaction of IR radiation with matter (probably, by radiation scatter on heterogeneities of the sample). Note that the use of polynomials of higher powers (quadratic and cubic) for the generation of differential spectra does not improve the statistical parameters characterizing regression.

Under visual comparison, the spectra of the racemate and enantiomerically pure crystalline samples of the two first members of the series **1a,b** differ noticeably, whereas for the three last members (**1c–e**) they coincide in detail (Fig. 1). A similar pattern is observed for the differential curves: in the case of compounds **1c–e**, differences between the spectra of the racemates and enantiomerically pure samples are at the level of instrumental background, while they are rather substantial for compounds **1a,b**. This agrees with an assumption that racemic substances are formed upon crystallization of racemic H- and F-substituted derivatives and racemic conglomerates are formed by the Cl-, Br-, and I-substituted derivatives, although cannot be considered as the final proof of this phenomenon.

Useful information on the type of melting of chiral compounds can be obtained by comparison of melting points of enantiomerically pure and racemic samples. The racemic conglomerates have a much lower melting temperature. However, the experimental melting points of the racemic samples of the simplest aromatic glycerol ethers differ considerably. For instances, the database²¹ contains 25 references to the melting points of racemic phenoxy derivative **1a**, which overlap the interval from 43 to 70 °C. Three references represent the melting points of racemic *o*-fluorosubstituted derivative **1b** from 37 to 57 °C. Our experience, which is presented in part in Experimental, completely confirms this feature. The racemic samples of diols **1a–e** with almost equal chemical purity (GC-MS monitoring found no chemical contamination) melted in variable but always broad temperature intervals (visual monitoring). As a rule, the samples subjected to the most thorough "purification" and consisting of larger, well formed grains melt in a wider interval shifted to higher temperatures. This specific feature is not characteristic of scalemic compounds **1a–e** with a high content of one of the enantiomers, whose samples possess sharp melting points under visual monitoring.

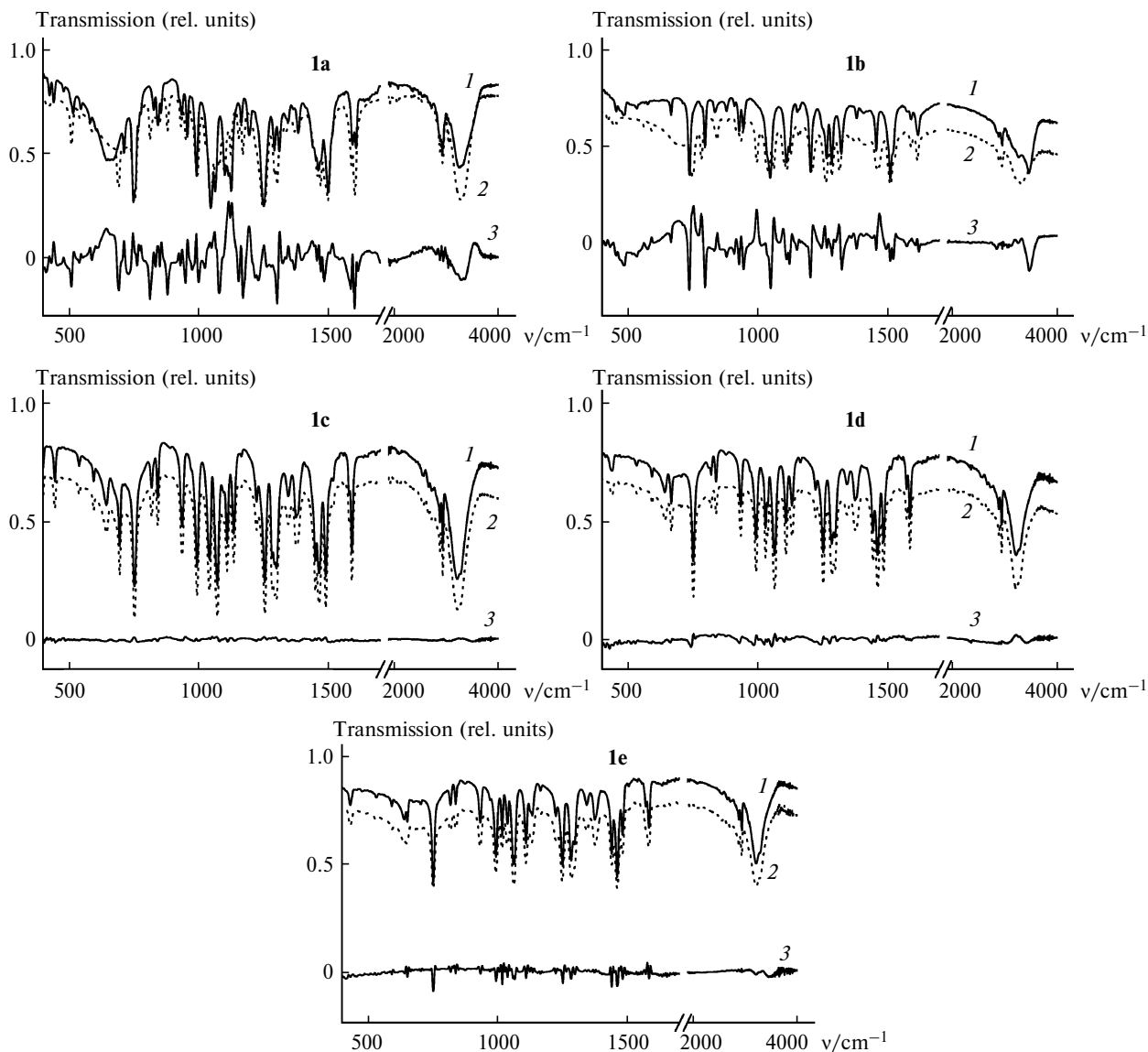


Fig. 1. IR spectra of solid samples **1a–e**: racemate (1), individual enantiomer (2), and differential spectrum (3).

Differential scanning calorimetry confirms the difference between the character of melting of the racemates and enantiomerically pure samples. The experimental melting curves for compounds **1a–e** with high (> 99%) enantiomeric excess are shown in Fig. 2.

As can be seen from the data in Fig. 2, the melting of enantiomerically pure diols is described by narrow sharp curves with a steep linear frontal edge (specific features of interpretation of the thermographic curves are discussed below). The typical experimental melting curves for the high-purity samples of racemic diols **1a,b**, which were obtained directly after recrystallization, are presented in Fig. 3 for comparison. These thermograms are far from ideality and represent a broad flat curve without a pronounced maximum (see Fig. 3, curve 1) or a polymodal curve (see Fig. 3, curve 2). These thermograms do not

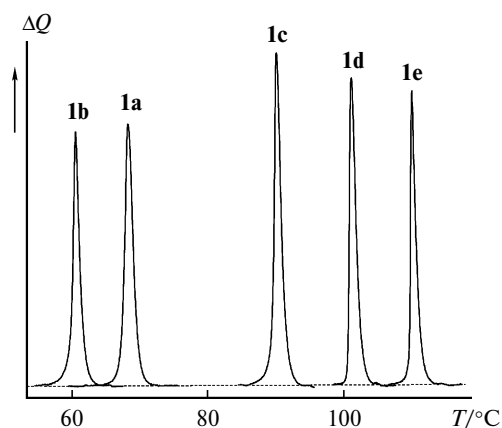


Fig. 2. Melting curves for samples of compounds **1a–e** with high enantiomeric purity.

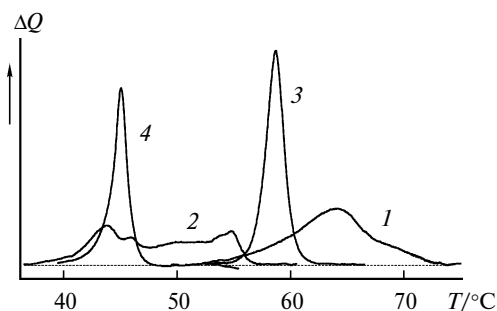


Fig. 3. Melting curves for pure samples of racemic diols: the starting coarse-crystalline samples *rac-1a* (1) and *rac-1b* (2) and finely ground samples *rac-1a* (3) and *rac-1b* (4).

allow one to characterize the "melting" of the samples by a single temperature and a reproducible enthalpy value of the process.

The shape of the experimental DSC curves changed dramatically (see Fig. 3, curves 3 and 4), when the samples of racemic diols **1a,b** were thoroughly ground before placing into the calorimeter cell. The qualitative change in the shape of the curves caused by mechanical grinding suggests that the unusual behavior of racemic glycerol ethers on melting is caused by a change in the character of processes accompanying the destruction of the crystal lattice upon the interaction with the liquid phase rather than by changes in the crystal lattice. Although curves 3 and 4 in Fig. 3 retain a substantial width, they can be characterized by a distinct maximum (melting point) and integrated reproducibly (*i.e.*, the enthalpy of the process can be measured). Therefore, the DSC data for these samples can be used to construct phase diagrams for melting of chiral aryloxypropanediols **1**.

The heterogeneous equilibrium between condensed phases in binary systems of enantiomers, which is reflected by these diagrams, can be complicated by polymorphism (existence of different crystalline phases of the same composition), temperature-dependent polymorphic transitions, and partial or complete miscibility of solid phases (formation of zones of solid solutions).²² It is more difficult to construct and analyze the phase diagrams because of this behavior, which, however, is rather rare. In the most cases, melting/crystallization of a binary mixture of enantiomers can be reduced to two idealized cases: solid-state formation of a racemic conglomerate or a racemic substance.^{19,20} In the first case, the binary phase diagram of melting is V-shaped with the single eutectic corresponding to the 1 : 1 ratio of enantiomeric components. The symmetric liquidus lines of this diagrams are described by the simplified Schröder—Van Laar equation, which is usually used for binary systems forming no molecular compounds in the solid phase,¹⁹

$$\ln x = \frac{\Delta H_A^f}{R} \left(\frac{1}{T_A^f} - \frac{1}{T^f} \right), \quad (1)$$

where x is the mole fraction of one of the enantiomers in the mixture (the mole fraction of another enantiomer is $x' = 1 - x$); ΔH_A^f (J mol⁻¹) and T_A^f (K) are the enthalpy of melting and melting point of the pure enantiomers; R is the universal gas constant ($R = 8.3170$ J K⁻¹ mol⁻¹).

The phase diagram for a racemic substance is W-shaped and characterized by two eutectics with the compositions $m : n$ and $n : m$. In this case, the liquidus line in the terminal regions is described by Eq. (1), and its central fragment obeys the Prigogine—Defay equation,²³ which is usually used in the simplified form

$$\ln[4x(1-x)] = \frac{2\Delta H_R^f}{R} \left(\frac{1}{T_R^f} - \frac{1}{T^f} \right), \quad (2)$$

where ΔH_R^f (J mol⁻¹) and T_R^f (K) are the enthalpy of melting and melting point of a racemic compound, and other designations are the same as in Eq. (1).

Thus, in the idealized case, to construct the liquidus of the phase diagram for melting of a conglomerate-forming substance, it is enough to have data on the melting temperature and enthalpy of melting for an enantiomerically pure sample. Additional data on the enthalpy and melting point of a racemate are needed to construct (in a similar approximation) the liquidus of a chiral substance forming a racemic compound. In both cases, the theoretical solidus line is a straight line parallel to the abscissa and passing through the point (points) of eutectic melting. The latter are found as a combined solution (intersection point) for different branches of the liquidus line.

The temperature and enthalpy of the thermally initiating process (in particular, melting) can be determined experimentally by the DSC method. If melting is described by the single peak, then its enthalpy is unambiguously determined by the surface area (integral) of this peak. The choice of the temperature of the process is rather arbitrary. In our constructions, we followed the recommendations of the German Society for Thermal Analysis (GEFTA)²⁴ and methodological instructions in Ref. 25. For a pure substance, whose melting is not complicated by additional processes, the melting peak looks like a narrow triangle with the virtually linear frontal and back edges (Fig. 4, curves 1, 1'). In this case, the intersection point of the baseline and frontal edge forming the γ angle with the baseline is taken as the melting point. Ideally, this angle is constant for a given instrument and specified conditions of thermogram recording. In practice, this constant is determined from melting curves of standard samples (in our case, these are twice sublimed phenol and naphthalene). The shape of the melting curve of the sample under study can differ strongly from ideality and be polymodal (see Fig. 4, curve 3). However, in the case of the real unimodal curve (see Fig. 4, curve 2), its frontal edge contains nonlinear regions and the slope angle

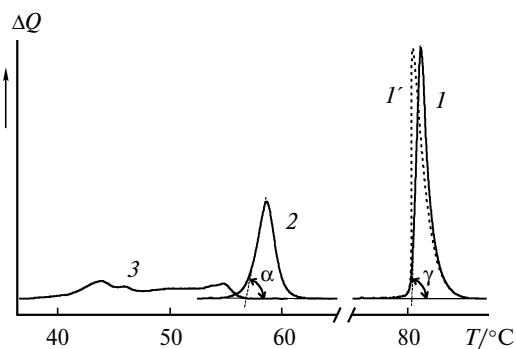


Fig. 4. Typical melting curves: I and I' , standard (naphthalene) before (I) and after the correction procedure (deconvolution, I'); 2 , unimodal curve with a distorted frontal edge (*rac-1a*); 3 , polymodal curve (*rac-2b*, large crystals).

of the linear region of the edge to the baseline α does not coincide with the γ angle ($\alpha \leq \gamma$).

Following the known recommendations,^{24,25} we accepted the intersection point of the line dropped from the maximum of the curve to the baseline at the γ angle (T_L) as the temperature of melting termination. To facilitate the visual perception of experimental results, we took into account the standard slope (γ) beforehand. For this purpose, the temperature scale was corrected to the equation $t' = t - h \cdot \cot(\gamma)$, where t is the observed temperature, t' is the corrected temperature, and h is the thermal flux for the given point. After this deconvolution of the experimental curves, the frontal edge of an ideal sample forms the right angle with the baseline, and the melting temperature T_L corresponds to the maximum in the curve. These curves are shown in Figs 2 and 3. The experimental data on the melting points and enthalpies of melting for racemic and enantiomerically pure samples **1a–e** are given in Table 1. When plotting experimental phase diagrams for binary mixtures of enantiomers, it is important to have reliable data on the enantiomeric composition of the sample under study (mole fractions x_R and x_S of each enantiomer, $x_R + x_S = 1$). For this purpose, we used the optical purity value $op = [\alpha_i]/[\alpha_{\max}] \approx ee = |x_R - x_S|/(x_R + x_S)$. The higher is the enantiomeric purity

of the sample, whose specific rotation value is used as the parameter $[\alpha_{\max}]$, the more the op value approaches to the true enantiomeric excess ee . The used combined GC-MS and thermographic monitoring warrants the chemical and enantiomeric purity of reference samples of all diols studied to be at least 99%.

The liquidus lines of the phase diagrams for these compounds, which were calculated by Eq. (1) and experimental data for enantiomerically pure diols, are presented in Fig. 5 by dashed lines. The same figures show the experimentally obtained liquidus points drawn by circles. For samples of diols **1a–e** with an intermediate enantiomeric composition, the experimental DSC thermograms sometimes contain additional peaks with the almost constant (for a certain compound) temperature T_{eu} , which corresponds to the melting point of the eutectics. These experimental characteristics are put on the plot as solid circles.

As can be seen from the data in Figs 5, *a–e* for the three last members of the series, *viz.*, *o*-Cl-, *o*-Br-, and *o*-I-substituted derivatives, the experimental points virtually fall on the line of the theoretical phase diagrams calculated by Eq. (1) for the conglomerate-forming compound. The calculated temperatures of eutectic melting for these compounds coincide almost exactly with the melting point of the racemate (see Table 1). In the case of F-substituted derivative **1b**, a discrepancy of ~ 7 °C is observed, which increases to 12 °C for unsubstituted derivative **1a**. The liquidus branches corresponding to Eq. (2) were calculated and are shown in the figures (dotted lines) for these two compounds. A comparison of thus obtained theoretical phase diagrams with experiment shows undoubtedly that phenoxypropanediol **1a** forms the typical racemic substance on crystallization. The same concerns, most likely, diol **1b**.

Knowing the melting temperature and enthalpy of melting for racemate and individual stereoisomers makes it possible to consider thermodynamic characteristics, which cannot directly be determined experimentally, for analysis of the type of crystallization. For instance, in the ideal case, the entropy of mixing of individual enantiomers ΔS_1^m in the liquid phase for the racemic conglomerate

Table 1. Thermodynamic characteristics of 3-(2-R-phenoxy)propane-1,2-diols*

| R | T_A^f | T_R^f | ΔT_{A-R}^f | T_{eu}^f | ΔH_A^f | ΔH_R^f | $\Delta G_{T_R^f}^0$ | ΔS_1^m |
|----|---------|---------|--------------------|-------------|----------------|----------------|----------------------|----------------|
| | °C | | | | | | | |
| H | 68.2 | 58.7 | 9.5 | 46.2 (56.0) | 28600 | 26330 | -1116 | 2.30 |
| F | 60.5 | 45.0 | 15.5 | 37.6 (43.9) | 26040 | 20500 | -623 | 3.39 |
| Cl | 90.0 | 71.7 | 18.3 | 71.1 | 38150 | 29000 | -64 | 4.90 |
| Br | 101.1 | 80.3 | 20.8 | 80.3 | 38380 | 33390 | 4 | 5.51 |
| I | 110.4 | 89.3 | 21.1 | 89.0 | 37380 | 34220 | -31 | 5.42 |

* The eutectic melting temperatures calculated for the racemic conglomerate and racemic compound (in parentheses) are presented.

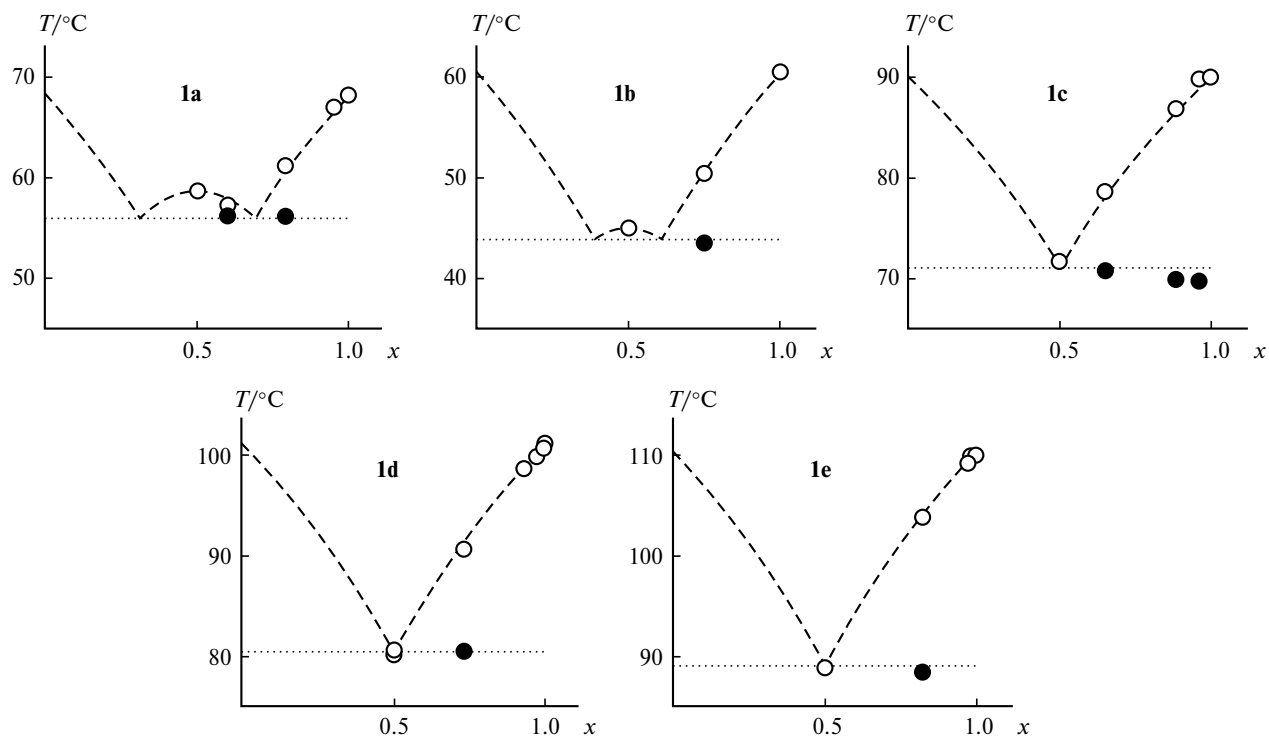


Fig. 5. Phase diagrams of binary mixtures of enantiomers of compounds **1a–e**; x is the mole fraction of the R -enantiomer.

ate is $R \cdot \ln 2 = 5.75 \text{ J mol}^{-1} \text{ K}^{-1}$, and the theoretical free energy ΔG_{TfR}^0 for racemic compound formation is always negative. These thermodynamic parameters can be calculated from the experimentally measured characteristics using Eqs (3) and (4), respectively.²⁶

$$-\Delta S_1^m = \frac{\Delta H_A^f}{T_A^f} - \frac{\Delta H_R^f}{T_R^f} - \frac{\Delta H_A^f - \Delta H_R^f}{T_A^f - T_R^f} \ln \frac{T_A^f}{T_R^f} \quad (3)$$

$$\Delta G_{TfR}^0 = - \frac{(T_R^f - T_A^f) \Delta H_A^f}{T_A^f} - T_R^f R \ln 2 \quad (4)$$

We estimated the error of determination of ΔS_1^m and ΔG_{TfR}^0 by the Monte Carlo method on the basis of the data on the measurement error for T^f and ΔH^f of standard substances. We took 5% of the measured enthalpy value and 0.5 °C for the melting temperature as estimates of these errors. Using these parameters, a pseudo-random selection of 1000 points was generated, and ΔS_1^m and ΔG_{TfR}^0 were calculated and root-mean-square deviations, which were accepted as estimates of the determination error of ΔS_1^m and ΔG_{TfR}^0 , were estimated on the basis of these points. Their values were $0.17 \text{ J mol}^{-1} \text{ K}^{-1}$ and 70 J mol^{-1} , respectively.

The calculated ΔS_1^m and ΔG_{TfR}^0 values for the compounds under study are also presented in Table 1. The considerable negative value of ΔG_{TfR}^0 for 3-phenoxypropane-1,2-diol (**1a**) indicates that the formation of a racemic substance in the solid phase is thermodynamically preferential. The ΔS_1^m value shows substantial devia-

tions from ideality when mixing individual stereoisomers of this substance. These deviations are related to preferential contacts between molecules of stereoisomers with different configurations. The thermodynamic characteristics of F-substituted derivative **1b** also indicate that a racemic compound is formed in the solid phase, although this compound is less stable than the unsubstituted one. For Cl-, Br-, and I-substituted compounds **1c–e**, the ΔS_1^m and ΔG_{TfR}^0 values are close for all the three substances and fall in the interval of values, which are typical of racemic conglomerates.

Thus, the study of the vibrational spectra and thermodynamic characteristics of five similar 3-(2- R -phenoxypropane)-1,2-diols revealed that in this series an increase in the substituent size primarily decreases the stability of racemic substances that are formed in the crystalline state. After some critical size is achieved, the type of crystallization of homologous chiral compounds changes, resulting in the formation of racemic conglomerates in the solid phase. Note that the change in the type of crystallization depending on the anion size has been observed earlier²⁷ for salts of chiral amino alcohols. Further analysis of the nature of crystallization, in the case under study, can be carried out by investigation of the microenvironment of chiral molecules in the crystal lattice. In addition, the observation of new conglomerates would extend the sphere of practical use of spontaneous resolution of racemates into individual enantiomers. Both these aspects (theoretical and applied) will be studied in the future.

The authors thank D. R. Sharafutdinova for performing GC-MS analysis.

This work was financially supported by the Russian Foundation for Basic Research (Project Nos 03-03-33084 and 06-03-32508).

References

1. A. A. Bredikhin, D. V. Savel'ev, Z. A. Bredikhina, A. T. Gubaidullin, and I. A. Litvinov, *Izv. Akad. Nauk, Ser. Khim.*, 2003, 812 [*Russ. Chem. Bull.*, 2003, **52**, 853 (Engl. Transl.)].
2. L. Pasteur, *Ann. Chim. Phys.*, 1848, **24**, 442; L. Pasteur, *Compt. Rend. Acad. Sci.*, 1848, **26**, 535.
3. A. Collet, M.-J. Brienne, and J. Jacques, *Chem. Rev.*, 1980, **80**, 215.
4. L. Perez-Garcia and D. B. Amabilino, *Chem. Soc. Rev.*, 2002, **31**, 342.
5. A. A. Bredikhin, Z. A. Bredikhina, S. N. Lazarev, and D. V. Savel'ev, *Mendeleev Commun.*, 2003, 104.
6. D. V. Zakharychev, M. D. Borisover, and B. N. Solomonov, *Zh. Fiz. Khim.*, 1995, **69**, 175 [*Russ. J. Phys. Chem.*, 1995, **69** (Engl. Transl.)].
7. Y. Gao, R. M. Hanson, J. M. Klunder, S. Y. Ko, H. Masamune, and K. B. Sharpless, *J. Am. Chem. Soc.*, 1987, **109**, 5765.
8. J. Chen and W. Shum, *Tetrahedron Lett.*, 1995, **36**, 2379.
9. G. Egri, A. Kolbert, J. Balint, E. Fogassy, L. Novak, and L. Poppe, *Tetrahedron Asymmetry*, 1998, **9**, 271.
10. K. Kitaori, Y. Furukawa, H. Yoshimoto, and J. Otera, *Tetrahedron*, 1999, **55**, 14381.
11. T. Toshikuni, S. Takeshi, and O. Hiromichi, *Tetrahedron Asymmetry*, 2001, **12**, 2001.
12. F. Theil, J. Weidner, S. Ballschuh, A. Kunath, and H. Schick, *J. Org. Chem.*, 1994, **59**, 388.
13. J. P. Lambooy, *J. Am. Chem. Soc.*, 1951, **73**, 349.
14. B. J. Ludwig, W. A. West, and W. E. Currie, *J. Am. Chem. Soc.*, 1952, **74**, 1935.
15. T. Seki, T. Takezaki, R. Ohuchi, M. Saitoh, T. Ishimori, and K. Yasuda, *Chem. Pharm. Bull.*, 1995, **43**, 1719.
16. GB Pat. 628497; *Chem. Abstrs.*, 1950, **44**, 3023d.
17. S. Kuwabe, K. Torraca, and S. Buchwald, *J. Am. Chem. Soc.*, 2001, **123**, 12202.
18. P. Brenans, *Bull. Soc. Chim. Fr.*, 1913, **13**, 533.
19. J. Jacques, A. Collet, and S. H. Wilen, *Enantiomers, Racemates, and Resolutions*, Krieger Publishing Co, Malabar, FL, 1994, 447 pp.
20. E. L. Eliel, S. H. Wilen, and L. N. Mander, *Stereochemistry of Organic Compounds*, John Wiley and Sons, New York, 1994, 1267 pp.
21. *Beilstein Database, Copyright©1988–2004*, Beilstein Institut zur Foerderung der Chemischen Wissenschaften licensed to Beilstein GmbH and MDL Information System GmbH, Beilstein GmbH, Frankfurt am Main, Germany.
22. G. Coquerel, *Enantiomer*, 2000, **5**, 481.
23. I. Prigogine and R. Defay, *Chemical Thermodynamics*, Longmans Green and Co, London—New York—Toronto, 1954.
24. G. W. H. Höhne, H. K. Cammenga, W. Eysel, E. Gmelin, and W. Hemminger, *Thermochim. Acta*, 1990, **160**, 1.
25. H. E. Gallis, F. Bougrioua, H. A. J. Oonk, P. J. van Ekeren, and J. C. van Miltenburg, *Thermochim. Acta*, 1996, **274**, 231.
26. Z. J. Li, M. T. Zell, E. J. Munson, and D. J. W. Grant, *J. Pharm. Sci.*, 1999, **88**, 337.
27. A. A. Bredikhin, Z. A. Bredikhina, A. T. Gubaidullin, D. B. Krivolapov, and I. A. Litvinov, *Mendeleev Commun.*, 2004, **14**, 268.

Received November 1, 2005